NJC

RSC Publishing

PAPER

View Article Online
View Journal | View Issue

Organogels from unsymmetrical π-conjugated 1,3,4-oxadiazole derivatives†

Cite this: *New J. Chem.*, 2013, **37**, 1454

Chengxiao Zhao,[a] Haitao Wang,[a] Binglian Bai,[b] Songnan Qu,[c] Jianxi Song,[a] Xia Ran,[a] Yan Zhang[a] and Min Li*[a]

Received (in Montpellier, France) 25th July 2012,
Accepted 13th February 2013

DOI: 10.1039/c3nj40648b

www.rsc.org/njc

In this study, the unsymmetrical π-conjugated gelators, 2-(3,4-bis(alkoxy)phenyl)-5-(pyridine-4-yl)-1,3,4-oxadiazole [4-POXD-B*n* (*n* = 4, 8, 12)], were synthesized and screened for gelation in various solvents. The tendencies of the critical gelation concentration (CGC) and the gel–sol phase transition temperatures (T_{gel}) of the 4-POXD-B8 gels, as well as the relationship between the end-chain length of gelator and gelation ability, indicated that the solvophobic effect has a critical role in gelation. For the specific gelator that we studied, we observed that the strength of the solvophobic force was related to the solvent properties. The solvent effect on gelation was studied quantitatively using the solvent polarity parameters: polar solubility parameter (δ_a), dielectric constant (ε), and polarity parameter ($E_T(30)$). The results revealed that the favorable δ_a domain and $E_T(30)$ domain for the gelation of 4-POXD-B8 was in the range of 8.1–12.6 (cal $cm^{-3})^{1/2}$ and 43.3–55.7 kcal mol^{-1}, respectively. Meanwhile, a decrease of δ_a and $E_T(30)$ in the solvents is unfavorable for gelation. Furthermore, the solvent effect on the microstructure of the gels was studied *via* scanning electron microscopy (SEM). The SEM images revealed that the gels from 4-POXD-B8 in DMSO and DMF were composed of helical ribbons, whereas those formed in other solvents consisted of flat ribbons.

Introduction

Low-molecular-mass organogels (LMOGs) are a new class of materials in supramolecular chemistry, in which organogelators spontaneously self-assemble through noncovalent interactions to create three-dimensional networks capable of entrapping solvents therein.[1] Different kinds of non-covalent interactions, such as hydrogen bonds, π-stacking, van der Waals, and the solvophobic effect, *etc.*, are involved in such supramolecular building.[2] Among the reported LMOGs, the π-conjugated LMOGs have drawn significant attention because of their potential application in optoelectronics.[3] At present, the structure–activity relationships that underpin self-assembly into gels are not fully understood. However, a new π-conjugated gelator can be synthesized by introducing *n*-alkyl chains, amide, or urea groups into the central π-conjugated cores, such as phthalocyanine,[4] acene,[5,6] anthracene,[6] perylene,[7,10] hexanbenzocoronene,[8] bisphenazine,[9] *etc.* The *n*-alkyl chains, amide, and urea groups direct the self-assembly and gelation of π-conjugated molecules through van deer Walls and hydrogen bonding interactions.[2,3] Hopf and co-workers have reported on the π-conjugated organogelator, 2,3-di-alkoxytetracenes, in which the π–π stacking and van der Waals interactions are the driving forces for the gelation.[6] Würthner *et al.* synthesized a urea-containing tetraphenoxy-substituted perylene bisimide gelator, forming a gel in toluene *via* self-assembly through hydrogen bonding and π–π stacking interactions.[10]

Recent studies have shown that solvents have an important role in the delicate equilibrium for gelation, aside from the influence of the gelator structure.[11,17] The simplest approach to quantifying solvent effects is to use solvent parameters, such as the dielectric constant (ε), Kamlet–Taft,[12] Hildebrand (δ), Reichardt's ($E_T(30)$),[13] and Hansen parameters (δ_d, δ_p, δ_h).[11] Hanabusa and co-workers have reported that the minimum gelation concentration of cyclo(dipeptide) gelators is dependent on the Hildebrand parameters of solvents.[14] Tritt-Goc and co-workers correlated the thermal gelation properties of the gels with different solvent parameters.[15] Furthermore, Smith and

[a] *Key Laboratory of Automobile Materials (Jilin University), Ministry of Education, Institute of Materials Science and Engineering, Jilin University, Changchun 130012, PR China. E-mail: minli@jlu.edu.cn*
[b] *College of Physics, Jilin University, Changchun 130012, PR China*
[c] *Key Laboratory of Excited State Processes, Changchun Institute of Optics, Fine Mechanics and Physics, Chinese Academy of Sciences, Changchun 130033, PR China*

† Electronic supplementary information (ESI) available: SEM images, gel photographs, solvent parameters, XRD and UV-vis spectra. See DOI: 10.1039/c3nj40648b

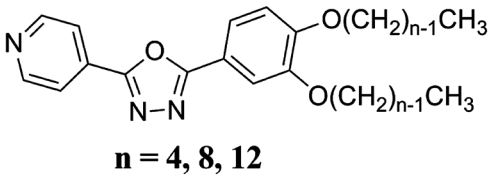

Scheme 1 Molecular structures of 4-POXD-B*n* (*n* = 4, 8, 12).

co-workers noticed that the Kamlet–Taft parameters, in particular α, can have a degree of predictive power for the gelation processes.[16] Jamart-Grégoire and co-workers established the relationship between the gel behavior of amino acid gelators and the hydrogen-bonding Hansen parameters.[17] These studied gelators have a common denominator, *i.e.*, gelator–gelator hydrogen bonding, indicating that the solvents can easily affect the gelation through solvent–geltor hydrogen bonding. The existence of solvent–gelator interactions has also been demonstrated for the gelator without hydrogen bonding. However, only a few studies have focused specifically on the influence of solvents on gelation. Thus, the current study investigates the influence of solvents on the gelation of π-conjugated gelators without gelator–gelator hydrogen bonding.

1,3,4-Oxadiazole derivatives (OXD) have gained widespread use as electron-transporting/hole-blocking materials, emitting layers in electroluminescent diodes and nonlinear optical materials because of the electron-deficient nature of their heterocycle, high photoluminescence quantum yield, and good thermal and chemical stabilities. In our previous study, we have reported a series of twin-tapered π-conjugated molecules, bi-1,3,4-oxadiazole derivatives (BOXD), and found that the 1,3,4-oxadiazole ring was fully conjugated with the adjacent phenylene groups and the face-to-face donor–acceptor interactions were beneficial to π-stacking.[18,19] In this context, we have designed and synthesized a series of unsymmetrical π-conjugated 1,3,4-oxadiazole gelators, 2-(3,4-bis(alkoxy)phenyl)-5-(pyridine-4-yl)-1,3,4-oxadiazole (4-POXD-B*n* (*n* = 4, 8, 12); in Scheme 1), which consisted of a rigid part and two flexible terminal alkoxyl chains. The π–π stacking, van der Waals interactions, and solvophobic effect are expected to be the driving forces for gelation. Moreover, a relationship between the gelation properties of the π-conjugated 1,3,4-oxadiazole gelators and solvents was established to better understand the solvent effect.

Results and disscusion

Gel properties of 4-POXD-B*n*

A certain solubility of a gelator in solvents is a prerequisite for gelation, whereas microphase segregation from dissolved solvents induces gelation, in which different types of intermolecular interactions underpin the self-assembly of the gelators. The new gelators (4-POXD-B*n*, *n* = 4, 8, 12) were screened for their gelation ability in different types of solvents, such as aromatic solvents, alkanes, chlorinated solvents, esters, ethers, ketones, alcohols, and other polar solvents (Table S1, ESI†). The results are listed in Table 1 and Table S1 (ESI†).

Table 1 Gelation properties of 4-POXD-B*n* (*n* = 4, 8, 12) in different solvents[a]

Solvents	4-POXD-B4	4-POXD-B8	4-POXD-B12
Methyl cyclohexane	S[b]	G[b]	G[b]
Methanol	WG[b]	G(5.01)	P[b]
Ethanol	WG[b]	G(6.12)[b]	P[b]
n-Propanol	S[b]	G(6.49)[b]	P[b]
n-Butanol	S[b]	G(12.4)[b]	G(9.79)[b]
Acetonitrile	S	G(4.95)	G(4.09)
Dimethylformamide	S	G(29.4)	G(16.3)
Dimethyl sulfoxide	S	G(3.34)	G(2.16)

[a] G = opaque gel; WG = weak gel that can change into a solution at room temperature at a concentration of 5.5×10^{-2} mol L^{-1}; P = precipitation; S = solution; the values in the brackets denote the CGC (10^{-3} mol L^{-1}). [b] Gel or precipitation formed at −20 °C.

The data shows that 4-POXD-B8 can dissolve in esters, ethers, aromatic, as well as chlorinated solvents and gel DMSO, DMF, acetonitrile, and alcohols. Most of the gelified solvents are polar solvents, indicating the importance of solvophobic interactions between the gelator and solvent. The only exception to this trend is methyl cyclohexane (MCH), which might involve strong π–π stacking interactions due to MCH being benign for π systems.[20] Furthermore, the critical gelation concentration (CGC) value of 4-POXD-B8 declined from 2.94×10^{-2} mol L^{-1} (DMF) to 4.95×10^{-3} mol L^{-1} (acetonitrile), and then to 3.34×10^{-3} mol L^{-1} (DMSO), as the solvent polarity varied. Fig. 1 shows the gel–sol phase transition temperatures (T_{gel}) plotted against the concentration of 4-POXD-B8. T_{gel} increased until a plateau region was reached (denoted by a concentration-independent T_{gel}) as the concentration increased. After changing the solvent, the value of the T_{gel} in the "plateau region" decreased from 44 °C (DMSO) to 39 °C (methanol), and then to 28.6 °C (ethanol). The tendencies of the CGC and T_{gel} in the "plateau region", which were in agreement with the compatibility of alkanes with the solvents,[21] indicated that the solvophobic effect was the main driving force for gelation.

4-POXD-B4 and 4-POXD-B12, with shorter alkoxyl chains and longer alkoxyl chains, respectively, compared to 4-POXD-B8,

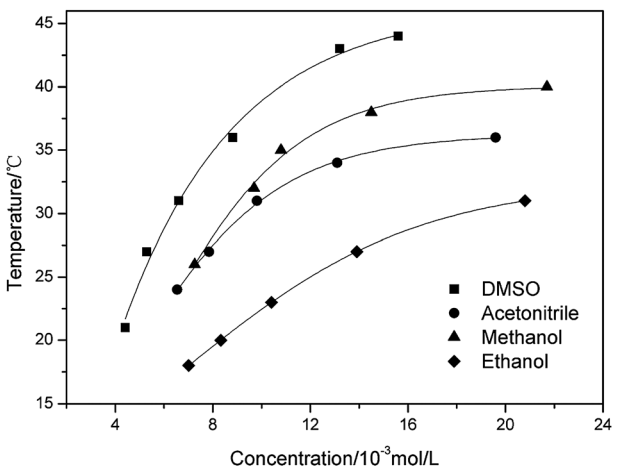

Fig. 1 Gel–sol phase-transition curves of 4-POXD-B8 in DMSO, acetonitrile, methanol, and ethanol.

were screened for gelation in these solvents to confirm the significance of the solvophobic effect in gelation (Table 1). 4-POXD-B4 formed weak gels in methanol and ethanol, and dissolved in DMSO and acetonitrile. Meanwhile, 4-POXD-B12 precipitated from methanol, ethanol, and *n*-propanol (Table 1), suggesting that the compatibility of the gelator with the solvents was weakened by lengthening the alkoxyl chains of the gelator; the length of the alkoxyl chains in 4-POXD-B8 was suitable for gelation.

Influence of the solvent on gelation

Based on the Gibbs energies of the solvation of alkanes in various solvents (Table S3, ESI†) reported by Solomonov *et al.*,[21] the strength of the solvophobic effects of the alkoxyl chains towards the solvents increased as the polarity of the solvents increased, such that solvents with a high polarity interacted with the alkoxyl chains weakly. Thus, the bulk polarity parameters of the solvents, such as the polar solubility parameter (δ_a),[22] dielectric constant (ε), and polarity parameter ($E_T(30)$), were chosen to investigate the solvent effect on gelation of 4-POXD-B*n* quantitatively. Table S2 (ESI†) summarizes the values of these parameters for the studied solvents.

First, the gel behaviors of 4-POXD-B*n* (n = 8, 12) were correlated with the solvent parameters. The behavior of 4-POXD-B8 defines a wide, favorable δ_a domain for gelation between 8.1 and 12.6 (cal cm^{-3})$^{1/2}$, at which only ''gel'' behaviors are observed, as shown in Fig. 2a. The ''precipitation'' or ''insoluble'' behaviors were observed above 12.6 (cal cm^{-3})$^{1/2}$, whereas the ''solution'' behaviors were noticeable below 8.1 (cal cm^{-3})$^{1/2}$, indicating that a moderate strength of the solvophobic effect is favorable for gelation. Similarily, 4-POXD-B12 defines a narrow δ_a domain for gelation between 8.1 and 9.6 (cal cm^{-3})$^{1/2}$, except for *n*-propanol. Fig. 2b shows the gelation behaviors *versus* the $E_T(30)$ graph. The $E_T(30)$ domains for the gelation of 4-POXD-B8 and 4-POXD-B12 were 43.3–55.7 kcal mol^{-1} and 43.3–50.4 kcal mol^{-1}, respectively. Further, the strength of the gels were correlated with the solvent parameters. The gelation number (GN), which gives the number of solvent molecules gelified per molecule of gelator,[23] is one of the most common criteria to evaluate the strength of a gel as well as the gel–sol phase transition temperature. Within each solvent class, the GN and T_{gel} values of the 4-POXD-B8 gels increased with an increase of δ_a in each solvent class (Table 2 and Fig. S4, ESI†).

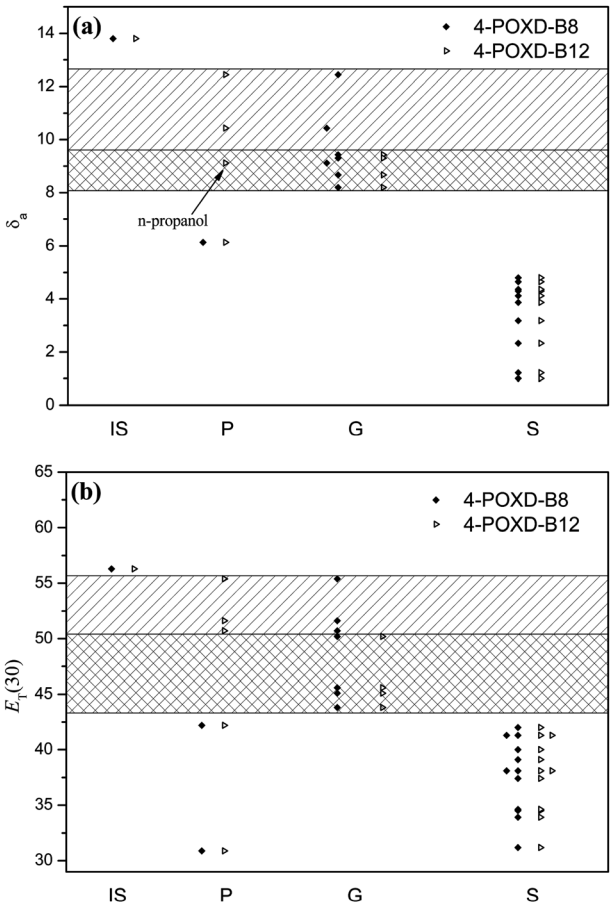

Fig. 2 Effect of the combined (a) polar solubility parameter δ_a and (b) polarity parameter $E_T(30)$ of the studied solvents on the gelation behaviors of 4-POXD-B*n* (n = 8, 12). G = gel; P = precipitation; S = solution; IS = insolubility.

Table 2 Bulk solvent parameters of the selected solvents: ε = dielectric constant, δ_a = polar solubility parameters, and $E_T(30)$ = polarity parameter. The T_{gel} is the gel–sol temperature for the studied gels with concentration of 1.32×10^{-2} mol L^{-1}

	δ_a/(cal cm^{-3})$^{1/2}$	ε	$E_T(30)$/kcal mol^{-1}	GN		T_{gel}/°C	
				4-POXD-B8	4-POXD-B12	4-POXD-B8	4-POXD-B12
DMSO	9.43	48.9	45.1	4219	6523	43	64
Acetonitrile	9.3	38.8	45.6	3859	4675	34	48
DMF	8.67	37.6	43.8	441	795	18	19
Methanol	12.44	33.62	55.4	4934	—	37	—
Ethanol	10.43	25.07	51.6	2799	—	26	—
n-Propranol	9.12	20.8	50.7	2056	—	17	—
n-Butanol	8.19	17.84	50.2	882	1121	16	—

Organogel structure

The xerogels were subjected to scanning electron microscopy (SEM) to examine the solvent effect on gel the microstructure. Fig. 3 shows the SEM images of the 4-POXD-B8 xerogels from different solvents. Flat and broad ribbons with a width of *ca.* 2 μm to 5 μm were observed in the 4-POXD-B8 xerogels from acetonitrile (Fig. 3a) and methanol (Fig. 3b). The xerogel from ethanol showed straight ribbons of 0.1 μm to 0.5 μm width (Fig. 3c). Interestingly, the 4-POXD-B8 xerogel from DMSO consisted of right- and left-handed helical ribbons with a width of 0.5 μm to 3 μm (Fig. 3d). In some cases, the wide helical ribbons were composed of several narrow ribbons. The helical pitches were non-uniform and both straight and flexible ribbons were observed, indicating that the helical structures did not come from the molecular chirality. The helical structures were also observed under an optical microscopic (OM), in which the ribbons exhibited periodical repetitions of bright and dark regions (Fig. 3f). Similar helical structures were also found in 4-POXD-B8 xerogels from DMF (Fig. 3e). The results clearly indicated that the solvent significantly

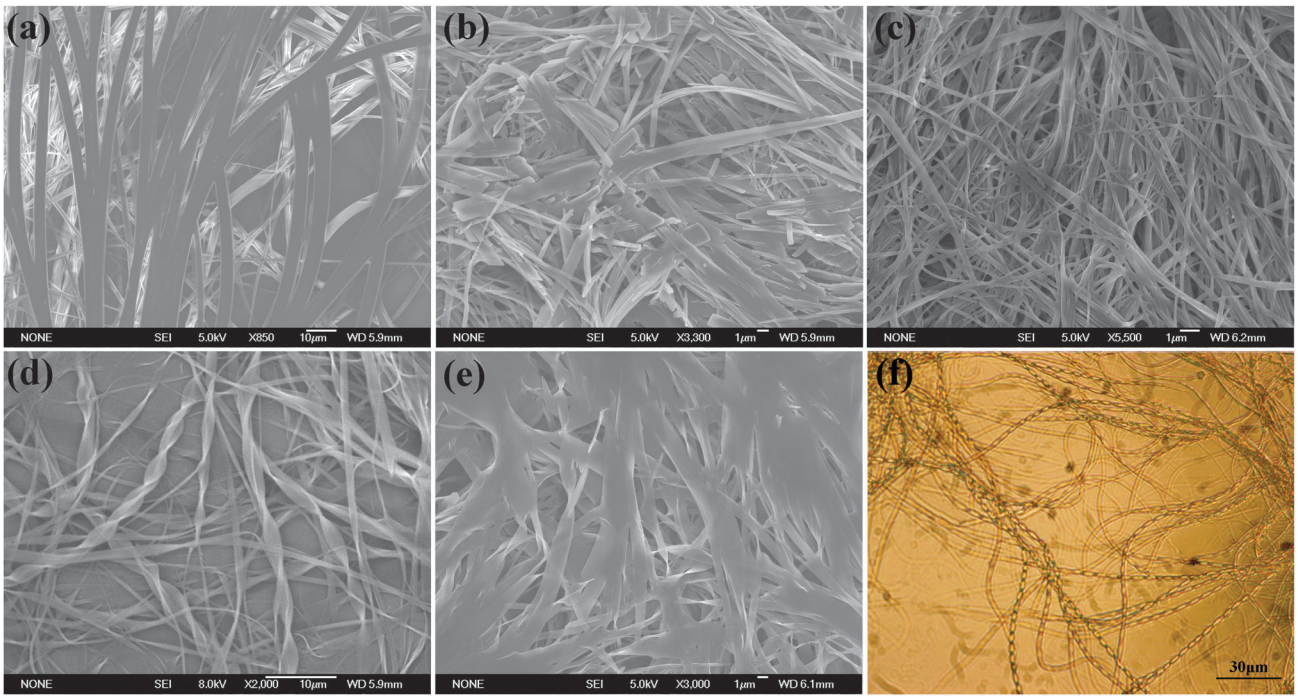

Fig. 3 SEM images of the 4-POXD-B8 xerogels from (a) acetonitrile, (b) methanol, (c) ethanol, (d) DMSO, and (e) DMF. (f) Optical microscopic image of the xerogel from DMSO.

affects the microstructure of the 4-POXD-B8 gels. The 4-POXD-B8 film casted from the dilute DMSO solution consisted of flat and flexible ribbons (Fig. S6, ESI†), whereas more ribbons, twisted nodes, and helical ribbons appeared with the increase in concentration. A similar phenomenon could be observed in the concentration-dependent DMF solutions of 4-POXD-B8 (Fig. S7, ESI†). This phenomenon indicates that the entanglement of ribbons may be one of the factors that cause the helical structure. The twisted fibers, which are much finer and denser, can be observed in the 4-POXD-B12 xerogel from DMSO (Fig. S8, ESI†).

The X-ray diffraction (XRD) patterns of the 4-POXD-B8 xerogels from different solvents exhibited several sharp diffraction peaks in the small- and high-angle regions, suggesting their crystalline features (Fig. 4). The slow evaporation of ethanol gave a precipitate showing a series of strong diffractions with *d*-spacings of 16.5 (11), 15.8 (20), and 12.8 Å (21) in the small-angle region, corresponding to the rectangular columnar structure with a = 31.7 Å and b = 19.4 Å. The XRD pattern of the 4-POXD-B8 xerogel from methanol shows two sets of diffractions; one set is similar to that of the precipitate from ethanol and the other set corresponds to the *d*-spacings of 39.4, 19.1, and 13.1 Å in the small-angle region. The *d*-spacing of 39.4 Å is nearly twice of the calculated full extended molecular length (*ca.* 20.5 Å) of 4-POXD-B8, indicating a bilayer structure. Similar structures were observed in the xerogels from DMSO and DMF (Fig. S9, ESI†). The 4-POXD-B8 xerogel form acetonitrile showed the first diffraction peak at a *d*-spacing of 27.1 Å (20.5 Å $< d <$ 41 Å), indicating that the 4-POXD-B8 molecules may have a large angle tilt in the bilayers (about 42°).

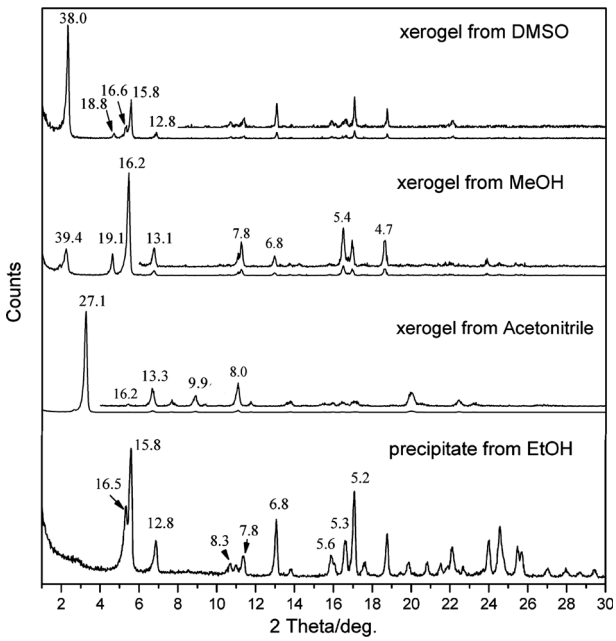

Fig. 4 X-Ray diffraction (XRD) spectra of the 4-POXD-B8 xerogels from DMSO, methanol, and acetonitrile.

Moreover, a bilayer structure was also observed in the 4-POXD-B12 xerogels (Fig. S10, ESI†).

Solvent-dependent optical properties of 4-POXD-B8

The optical properties of 4-POXD-B8 in various solvents are shown in Table 3. The shape (Fig. S11, ESI†) and position (Table 3) of the

Table 3 Photophysical properties of 4-POXD-B8 in various solvents (1×10^{-5} mol L^{-1}) at room temperature

Solvent	λ_{em}/nm	λ_{abs}/nm	Φ_F/%
Cyclohexane	351, 369, 384	315	80.7
Toluene	394	319	81.6
THF	425	318	64.9
DMF	458	317	73.3
DMSO	465	319	38.5
1-Butanol	460	321	11.2
1-Propanol	466	320	6.0
Ethanol	472	319	4.1
Methanol	479	318	0.5

absorbance maxima of 4-POXD-B8 are dependent on the solvent, indicating that the conjugation-structure of the 4-POXD-B8 molecule in its ground state changed with solvents.[24] In protic solvents, however, the absorbance maxima of 4-POXD-B8 blue-shifted from 321 nm (*n*-butanol) to 318 nm (methanol), suggesting the formation of solvent–solute hydrogen bonds. On the other hand, 4-POXD-B8 exhibited strong fluorescence with a vibronic structure in the apolar solvent cyclohexane and a weak broad fluorescence in polar solvents (Fig. S13, ESI†). The emission maxima red-shifted from 369 nm (in cyclohexane) to 465 nm (in DMSO) when the polarity of the solvent increased, and its fluorescence quantum yield (Φ_F) decreased from 80.7% (in cyclohexane) to 38.5% (in DMSO). This suggested the existence of intramolecular charge-transfer. The fluorescence quantum yields of 4-POXD-B8 in the aprotic solvents were markedly higher than that in the protic solvents, which may be due to solvent–solute hydrogen bonding.

Conclusion

This study reports the synthesis and gelation behaviors of a series of unsymmetrical π-conjugated gelators, 4-POXD-B*n* (*n* = 4, 8, 12). The 4-POXD-B8, with a moderate length of end-chains, can gel polar solvents, such as DMSO, acetonitrile, DMF, and alcohols. The tendencies of the CGC and T_{gel} indicate that the solvophobic effect is the driving force for gelation. Changing the length of the oxyalkyl chains in the gelators can induce a drastic change in the gelation properties, confirming that the solvophobic effect of the alkyoxyl chains towards the solvent dominates the gelation. The correlations between the gelation of 4-POXD-B*n* and the solvents were established using the solvent polarity parameters (δ_a, ε and $E_T(30)$). The favorable δ_a domain and $E_T(30)$ domain for the gelation of 4-POXD-B8 was in the range of 8.1–12.6 (cal $cm^{-3})^{1/2}$ and 43.3–55.7 kcal mol^{-1}, respectively. Thus, the capacity of a solvent to form a gel with our compounds can be predicted by the δ_a and $E_T(30)$ values. The GN and T_{gel} values of the gels increased with the increase of δ_a, ε, and $E_T(30)$. The SEM images revealed that the gels prepared from 4-POXD-B8 in DMSO and DMF are composed of helical ribbons, whereas those formed in other solvents consist of flat ribbons.

Experimental section

Characterization

^{1}H NMR and ^{13}C NMR spectra were recorded with a Mercury-300BB spectrometer, using tetramethylsilane (TMS) as an internal standard. X-ray diffraction was carried out with a Bruker Avance D8 X-ray diffractometer. Fourier transform infrared (FTIR) spectra were recorded with a Perkin-Elmer spectrometer (Spectrum One B). The sample was pressed into KBr pellets. The FTIR spectra of the xerogel samples were measured on a silicon wafer. Photoluminescence was measured on a Perkin-Elmer LS 55 spectrometer and the absorption measurements were recorded using a UV-2550 spectrometer. The UV-vis absorption spectrum in the gel state measured by casting a drop of concentrated solutions of 4-POXD-B8 on quartz. SEM observations were taken with a JSM-6700F apparatus. OM observation was conducted on a Leica DMLP optical microscope. The xerogel samples for SEM and OM measurements were prepared by dropping a small amount of gel on a silicon and glass wafer respectively, followed by lyophilization. The molecular length was calculated by MM2. The gel–sol phase transition temperatures were determined by the "falling drop" method.[25]

Syntheses

The synthesis of 4-POXD-B*n* (*n* = 4, 8, 12,) is outlined in Scheme 2. 3,4-Bis(alkoxy)benzoic acids (**1**) were prepared according to the literature[26] and the corresponding chlorides (**2**) were obtained by refluxing **1** with $SOCl_2$ for 8 h.[27] Compounds **2** were employed to react with equimolar isonicotinohydrazide in a 100 mL mixture of 1-methyl-2-pyrrolidinone (NMP) and THF at room temperature for 12 h. The solution was poured into 1000 mL distilled water and filtrated to obtain the white solid. The pure compounds of 4-PHP-B*n* recrystallized from ethanol were refluxed in $POCl_3$ for 30 h for the synthesis of 4-POXD-B*n* (*n* = 4, 8, 12).[28] The reaction mixtures were

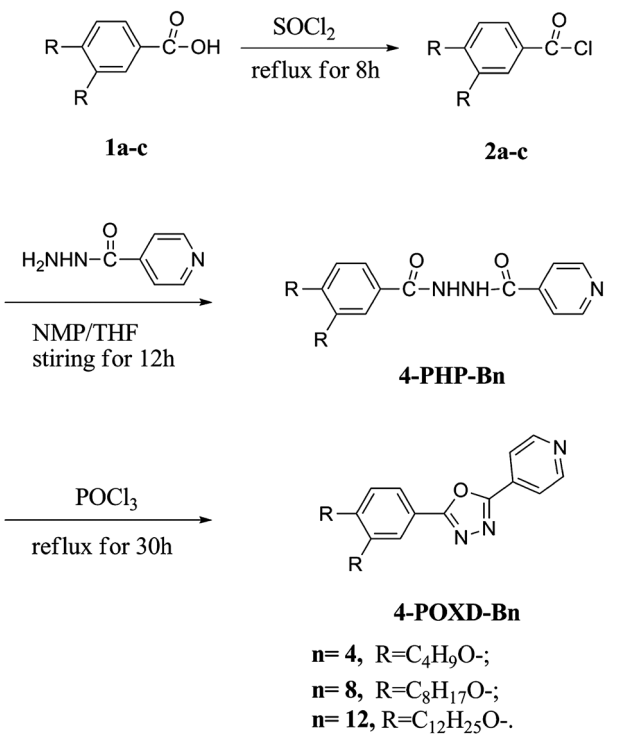

Scheme 2 Synthetic routes of 4-POXD-B*n* (*n* = 4, 8, 12).

gradually poured into 1000 mL distilled water and filtrated to obtain the yellow solid. The yellow solid was dried under vacuum and recrystallized from ethanol three times to give pure 4-POXD-B*n* gelators with a yield of more than 60%.

***N′*-(3,4-Bis(butoxy)benzoyl)isonicotinohydrazide (4-PHP-B4).** ^{1}H NMR (300 MHz, $CDCl_3$): δ ppm 10.23 (s, 1H), 9.43 (s, 1H), 8.78 (s, 2H), 7.80 (s, 2H), 7.43 (s, 1H), 7.40 (s, 1H), 6.84 (d, J = 8.1 Hz, 1H), 4.01 (m, 4H), 1.82 (m, 4H), 1.50 (m, 4H), 0.97 (m, 6H); FT-IR (KBr, pellet, cm^{-1}) ν: 3250, 3128, 3049, 3028, 2958, 2936, 2874, 2850, 1691, 1644, 1601, 1583, 1557, 1523, 1511, 1473, 1428, 1408, 1394, 1339, 1304, 1275, 1235, 1217, 1191, 1159, 1134, 1111, 1066, 1024, 1007, 968, 908, 873, 845, 813, 795, 749, 690, 615.

***N′*-(3,4-Bis(octyloxy)benzoyl)isonicotinohydrazide (4-PHP-B8).** ^{1}H NMR (300 MHz, $CDCl_3$): δ ppm 9.67 (d, J = 6.3 Hz, 1H), 9.14 (d, J = 5.1 Hz, 1H), 8.78 (dd, J = 4.5, 1.6 Hz, 2H), 7.70 (dd, J = 4.5, 1.6 Hz, 2H), 7.43 (d, J = 2.0 Hz, 1H), 7.39 (d, J = 2.0 Hz, 1H), 6.89 (d, J = 8.1 Hz, 1H), 4.04 (q, J = 6.7 Hz, 4H), 1.84 (m, 4H), 1.40 (m, 20H), 0.89 (m, 6H); FT-IR (KBr, pellet, cm^{-1}) ν: 3245, 3127, 3049, 3027, 2956, 2922, 2873, 2852, 1691, 1642, 1601, 1583, 1557, 1523, 1510, 1470, 1428, 1406, 1392, 1305, 1274, 1232, 1215, 1190, 1159, 1110, 1065, 1018, 999, 962, 908, 870, 844, 813, 748, 721, 690, 614.

***N′*-(3,4-Bis(dodecyloxy)benzoyl)isonicotinohydrazide (4-PHP-B12).** ^{1}H NMR (300 MHz, $CDCl_3$): δ ppm 9.68 (d, J = 6.4 Hz, 1H), 9.13 (d, J = 5.1 Hz, 1H), 8.78 (dd, J = 4.7, 1.6 Hz, 2H), 7.70 (dd, J = 4.6, 1.7 Hz, 2H), 7.43 (d, J = 2.1 Hz, 1H), 7.39 (d, J = 2.1 Hz, 1H), 6.88 (d, J = 8.2 Hz, 1H), 4.03 (q, J = 6.7 Hz, 4H), 1.84 (m, 4H), 1.39 (m, 36H), 0.88 (m, 6H); FT-IR (KBr, pellet, cm^{-1}) ν: 3243, 3130, 3050, 2954, 2920, 2870, 2849, 1689, 1642, 1602, 1583, 1557, 1520, 1511, 1470, 1429, 1406, 1393, 1379, 1305, 1274, 1233, 1215, 1191, 1160, 1110, 1065, 1018, 1000, 962, 910, 870, 844, 831, 813, 748, 722, 690, 652.

2-(3,4-Bis(butoxy)phenyl)-5-(pyridine-4-yl)-1,3,4-oxadiazole (4-POXD-B4). ^{1}H NMR (300 MHz, $CDCl_3$): δ ppm 8.86 (s, 2H), 8.04 (d, J = 4.8 Hz, 2H), 7.70 (d, J = 2.1 Hz, 1H), 7.66 (dd, J = 5.2, 2.0 Hz, 1H), 6.99 (d, J = 8.4 Hz, 1H), 4.11 (q, J = 6.5 Hz, 4H), 1.86 (m, 4H), 1.55 (m, 4H), 1.01 (m, 6H); ^{13}C NMR (75 MHz, $CDCl_3$): δ ppm 165.8, 162.2, 153.0, 150.2, 149.6, 131.8, 120.9, 120.4, 115.6, 113.1, 112.1, 69.3, 69.0, 31.3, 31.2, 19.2, 13.8; FT-IR (KBr, pellet, cm^{-1}) ν: 3055, 3039, 2958, 2934, 2874, 2851, 1608, 1593, 1571, 1552, 1538, 1500, 1468, 1446, 1411, 1394, 1339, 1320, 1280, 1255, 1222, 1149, 1111, 1066, 1024, 1008, 969, 864, 828, 802, 740, 723, 699. Anal. For $C_{21}H_{25}N_3O_3$, Found: C, 68.91; H, 6.94; N, 11.40. Calcd: C, 68.64; H, 6.86; N, 11.44.

2-(3,4-Bis(octyloxy)phenyl)-5-(pyridine-4-yl)-1,3,4-oxadiazole (4-POXD-B8). ^{1}H NMR (300 MHz, $CDCl_3$): δ ppm 8.85 (d, J = 5.9 Hz, 2H), 8.04 (dd, J = 4.7, 1.4 Hz, 2H), 7.70 (d, J = 2.0 Hz, 1H), 7.66 (dd, J = 6.5, 2.0 Hz, 1H), 6.99 (d, J = 8.3 Hz, 1H), 4.10 (q, J = 6.5 Hz, 4H), 1.88 (m, 4H), 1.43 (m, 20H), 0.89 (t, J = 6.8 Hz, 6H); ^{13}C NMR (75 MHz, $CDCl_3$): δ ppm 165.7, 162.3, 152.9, 150.7, 149.6, 131.4, 120.8, 120.3, 115.7, 113.2, 112.1, 69.6, 69.3, 31.8, 29.4, 29.3, 29.2, 29.1, 26.1, 26.0, 22.6, 14.1; FT-IR (KBr, pellet, cm^{-1}) ν: 3082, 3039, 2955, 2940, 2924, 2869, 2856, 1604, 1571, 1556, 1539, 1509, 1478, 1410, 1398, 1378, 1334, 1318, 1276, 1254, 1219, 1140, 1110, 1082, 1065, 1030, 989, 974, 886, 856, 831, 802, 739, 722, 702; Anal. For $C_{29}H_{41}N_3O_3$, Found: C, 72.62; H, 8.62; N, 8.76. Calcd: C, 72.79; H, 8.78; N, 8.84.

2-(3,4-Bis(dodecyloxy)phenyl)-5-(pyridine-4-yl)-1,3,4-oxadiazole (4-POXD-B12). ^{1}H NMR (300 MHz, $CDCl_3$): δ ppm 8.85 (dd, J = 4.6, 1.6 Hz, 2H), 8.07 (dd, J = 4.6, 1.6 Hz, 2H), 7.70 (d, J = 2.1 Hz, 1H), 7.66 (dd, J = 6.6, 2.0 Hz, 1H), 6.99 (d, J = 8.4 Hz, 1H), 4.10 (q, J = 6.5 Hz, 4H), 1.87 (m, 4H), 1.42 (m, 36H), 0.88 (t, J = 6.7 Hz, 6H); ^{13}C NMR (75 MHz, $CDCl_3$): δ ppm 165.8, 162.2, 153.0, 150.3, 149.6, 131.7, 120.9, 120.4, 115.6, 113.2, 112.1, 69.6, 69.3, 31.9, 29.7, 29.6, 29.4, 29.3, 29.2, 29.1, 26.1, 26.0, 14.1; FT-IR (KBr, pellet, cm^{-1}) ν: 3086, 2954, 2919, 2865, 2849, 1602, 1572, 1555, 1537, 1508, 1498, 1466, 1446, 1410, 1391, 1377, 1336, 1277, 1252, 1221, 1139, 1111, 1066, 1030, 993, 977, 923, 856, 824, 809, 739, 723, 700; Anal. For $C_{37}H_{57}N_3O_3$, Found: C, 75.08; H, 9.71; N, 7.10. Calcd: C, 75.14; H, 9.77; N, 6.99.

Acknowledgements

The authors are grateful to the National Science Foundation Committee of China (project no. 51073071, 51103057, 21072076), and Project 985-Automotive Engineering of Jilin University for their financial support of this work.

Notes and references

1 (*a*) P. Terech and R. G. Weiss, *Chem. Rev.*, 1997, **97**, 3133–3159; (*b*) D. J. Abdallah and R. G. Weiss, *Adv. Mater.*, 2000, **12**, 1237–1247; (*c*) N. M. Sangeetha and U. Maitra, *Chem. Soc. Rev.*, 2005, **34**, 821–836; (*d*) P. Dastidar, *Chem. Soc. Rev.*, 2008, **37**, 2699–2715.

2 (*a*) R. E. Melendez, A. J. Carr, B. R. Linton and A. D. Hamilton, *Struct. Bonding*, 2000, **96**, 31–61; (*b*) T. Ishi-i and S. Shinkai, *Top. Curr. Chem.*, 2005, **258**, 119–160; (*c*) F. Lerouge, G. Cerveau and R. J. P. Corriu, *New J. Chem.*, 2006, **30**, 1364–1376; (*d*) A. Hahma, S. Bhat, K. Leivo, J. Linnanto, M. Lahtinen and K. Rissanen, *New J. Chem.*, 2008, **32**, 1438–1448; (*e*) M. Boiani, A. Baschieri, C. Cesari, R. Mazzoni, S. Stagni, S. Zacchini and L. Sambri, *New J. Chem.*, 2012, **36**, 1469–1478.

3 K. Jang, A. D. Ranasinghe, C. Heske and D.-C. Lee, *Langmuir*, 2010, **26**, 13630–13636.

4 (*a*) D. D. Díaz, J. J. Cid, P. Vázquez and T. Torres, *Chem.–Eur. J.*, 2008, **14**, 9261–9273; (*b*) H. Engelkamp, S. Middelbeek and R. J. M. Nolte, *Science*, 1999, **284**, 785–788.

5 (*a*) J.-L. Pozzo, G. M. Clavier and J.-P. Desvergne, *J. Mater. Chem.*, 1998, **8**, 2575–2577; (*b*) M. Lescanne, A. Colin, O. Mondain-Monval, F. Fages and J.-L. Pozzo, *Langmuir*, 2003, **19**, 2013–2020; (*c*) J.-P. Hong, M.-C. Um, S.-R. Nam, J.-I. Hong and S. Lee, *Chem. Commun.*, 2009, 310–312.

6 J. Reichwagen, H. Hopf, A. Del Guerzo, C. Belin, H. Bouas-Laurent and J.-P. Desvergne, *Org. Lett.*, 2005, **7**, 971–974.

7 (*a*) K. Sugiyasu, N. Fujita and S. Shinkai, *Angew. Chem., Int. Ed.*, 2004, **43**, 1229–1233; (*b*) X.-Q. Li, V. Stepanenko, Z. Chen, P. Prins, L. D. A. Siebbeles and F. Würthner, *Chem. Commun.*, 2006, 3871–3873.

8 X. Dou, W. Pisula, J. Wu, G. J. Bodwell and K. Müllen, *Chem.–Eur. J.*, 2008, **14**, 240–249.
9 D.-C. Lee, K. K. McGrath and K. Jang, *Chem. Commun.*, 2008, 3636–3638.
10 F. Würthner, B. Hanke, M. Lysetska, G. Lambright and G. S. Harms, *Org. Lett.*, 2005, **7**, 967–970.
11 R. Wang, C. Geiger, L. Chen, B. Swanson and D. G. Whitten, *J. Am. Chem. Soc.*, 2000, **122**, 2399–2400.
12 B. Valeur, *Molecular Fluorescence: Principles and Applications*, Wiley-VCH Verlag GmbH, 2001.
13 *Polymer Handbook*, ed. J. Branderup, E. H. Immergut, E. A. Grulke, A. Abe and D. R. Bloch, John Wiley & Sons, New York, 4th edn, 1999; 2005.
14 K. Hanabusa, M. Matsumoto, M. Kimura, A. Kakehi and H. Shirai, *J. Colloid Interface Sci.*, 2000, **224**, 231–244.
15 (*a*) M. Bielejewski, A. Łapiński, R. Luboradzki and J. Tritt-Goc, *Langmuir*, 2009, **25**, 8274–8279; (*b*) M. Bielejewski, A. Łapiński, J. Kaszyńska, R. Luboradzki and J. Tritt-Goc, *Tetrahedron Lett.*, 2008, **49**, 6685–6689; (*c*) M. Bielejewski, A. Łapiński, R. Luboradzki and J. Tritt-Goc, *Tetrahedron*, 2011, **67**, 7222–7230.
16 W. Edwards, C. A. Lagadec and D. K. Smith, *Soft Matter*, 2011, **7**, 110–117.
17 P. Curcio, F. Allix, G. Pickaert and B. Jamart-Grégoire, *Chem.–Eur. J.*, 2011, **17**, 13603–13612.
18 S. N. Qu, L. J. Zhao, Z. X. Yu, Z. Y. Xiu, C. X. Zhao, P. Zhang, B. H. Long and M. Li, *Langmuir*, 2009, **25**, 1713–1717.
19 S. N. Qu, X. F. Chen, X. Shao, F. Li, H. Y. Zhang, H. T. Wang, P. Zhang, Z. X. Yu, K. Wu, Y. Wang and M. Li, *J. Mater. Chem.*, 2008, **18**, 3954–3964.
20 (*a*) M. R. Molla, A. Das and S. Ghosh, *Chem.–Eur. J.*, 2010, **16**, 10084–10093; (*b*) M. R. Molla, A. Das and S. Ghosh, *Chem. Commun.*, 2011, **47**, 8934–8936.
21 L. A. Sedov, M. A. Stolov and B. N. Solomonov, *J. Phys. Org. Chem.*, 2011, **24**, 1088–1094.
22 A. R. Hirst and D. K. Smith, *Langmuir*, 2004, **20**, 10851–10857.
23 G. Zhu and J. S. Dordick, *Chem. Mater.*, 2006, **18**, 5988–5995.
24 R. Hu, S. Li, Y. Zeng, J. Chen, S. Wang, Y. Li and G. Yang, *Phys. Chem. Chem. Phys.*, 2011, **13**, 2044–2051.
25 D. j. Abdallah and R. G. Weiss, *Langmuir*, 2000, **16**, 352–355.
26 (*a*) Y. D. Zhang, K. G. Jespersen, M. Kempe, J. A. Kornfield, S. Barlow, B. Kippelen and S. R. Marder, *Langmuir*, 2003, **19**, 6534; (*b*) E. Terazzi, S. Torelli, G. Bernardinelli, J. P. Rivera, J. M. Benech, C. Bourgogne, B. Donnio, D. Guillon, D. Imbert, J. C. G. Bunzli, A. Pinto, D. Jeannerat and C. Piguet, *J. Am. Chem. Soc.*, 2005, **127**, 888–903.
27 J. S. Dave and R. A. Vora, *Liquid Crystals and Ordered Fluids*, Plenum, New York, 1970, p 477.
28 S. N. Qu and M. Li, *Tetrahedron*, 2007, **63**, 12429–12436.

